ELSEVIER

Journal of Neuroscience Methods 94 (1999) 19–26

JOURNAL OF NEUROSCIENCE METHODS

www.elsevier.com/locate/jneumeth

# Miniature carrier with six independently moveable electrodes for recording of multiple single-units in the cerebellar cortex of awake rats

Bart P. Vos *, Mike Wijnants, Sofie Taeymans, Erik De Schutter

*Laboratory Theoretical Neurobiology, Born-Bunge Foundation, University of Antwerp, Universiteitsplein 1, B-2610 Antwerp, Belgium*

Received 13 July 1999; accepted 6 August 1999

**Abstract**

Ensemble recording in cerebellar cortex of awake rats presents unique methodological challenges not encountered when recording from the cerebral cortex or from deep brain structures with more homogeneous cell populations. Compared to the cerebral cortex, removal of dura over the cerebellum evokes pronounced swelling, and insertion of multiple closely spaced electrodes in the cerebellar cortex causes considerable dimpling (Welsh JP, Schwartz C. Multielectrode recording from the cerebellum. In: Nicolelis MAL, editor. Methods for Neural Ensemble Recordings, CRC Methods in Neuroscience Series. Boca Raton, FL: CRC Press LLC, 1999, pp. 79–100). Also, a repetitious and well-defined neural circuit characterizes the cerebellar cortex across its entire surface. With conventional multi-electrode methods, such as chronically implanted bundles or arrays of microwires, the risk of disrupting the cerebellar cytoarchitecture is high. In most conventional multi-electrode systems, electrodes have rather low impedance and cannot be moved independently after implantation. These limitations make proper unit isolation, necessary to identify each of the recorded cerebellar units, very difficult. We designed a lightweight (14 g), miniature (base plate: $19 \times 23$ mm; total height: 16 mm) multi-electrode system to allow for the chronic implantation of six independently moveable sharp electrodes with high impedance, in the cerebellar cortex. The six electrodes are arranged in a $2 \times 3$ matrix (inter-electrode distance: 0.6 mm). At any time after the implantation the vertical position of each individual electrode can be adjusted by screwing spring-loaded electrode heads up or down. The system preserves the integrity of the cerebellar cytoarchitecture, and enables easy isolation and identification of individual cerebellar units in awake, freely moving rats. 

*Keywords:* Multi-electrode; Cerebellar; Rats

## 1. Introduction

The circuitry of cerebellar cortex is unique in its regularity and simplicity compared to, for example, the cerebral cortex (Ito, 1984). Unraveling cerebellar operations using ensemble recordings in awake animals might contribute to the understanding of much more complex circuits like those in cerebral cortex or in other brain regions. However, the heterogeneous cell population and specific cytoarchitecture of the cerebellar cortex also require that, when performing ensemble recordings, the identity of each of the recorded units can be determined. Some neurons of the cerebellar circuit, (e.g. Purkinje cells) can be properly and unambiguously identified based on the recorded waveform (simple and complex spikes). However, this is only possible if the units are sufficiently well discriminated (Welsh and Schwartz, 1999). Our own research focuses on the largest inhibitory neuron in the circuit, the Golgi cell (Vos et al., 1999a,b,c). We have described a number of physiological criteria to identify Golgi cells, recorded in anesthetized rats, based on wave form, spontaneous firing patterns and evoked responses (Vos et al., 1999a,b,c). Golgi cells are located in the granular layer of the cerebellar cortex. This implies that Golgi cell spikes, if they are encountered, will always be found on a noisy background consisting of granular multi-unit activity, (e.g. Vos et al., 1999a,b,c), which is much

* Corresponding author. Tel.: +32-38-202610; fax: +32-38-202669.

*E-mail address:* bart@bbf.uia.ac.be (B.P. Vos)

0165-0270/99/$ - see front matter 
PII: S0165-0270(99)00122-3

higher in awake than in anesthetized animals (Hartmann and Bower, 1998).

The recording of cerebellar ensembles thus requires an optimal signal-to-noise ratio in order to easily isolate and identify all simultaneously captured units. Two factors are important to achieve an optimal signal-to-noise ratio: electrode impedance and the distance of the electrode tip to the cell. Sharp metal microelectrodes with high impedance are very well suited for easy spike isolation provided that they can be lowered fairly close to the soma. However, conventional methods for ensemble recording in freely moving animals use fixed bundles of multiple microwires, (e.g. Nicolelis and Chapin, 1994; Wilson and McNaughton, 1996, see Moxon, 1999 for review). Platinum-iridium micro-wires have the advantage of being somewhat flexible, but they usually have very low impedance because of their relatively large surface. While low impedance is advantageous in terms of reducing movement-artifacts, it also leads to smaller spikes. The large exposed surface can hamper spike isolation and discrimination. In addition, the commercially available micro-wire bundles or arrays do not allow for the displacement of single wires after the implantation.

Attempts to use the standard micro-wire configurations to perform chronic recordings of cerebellar units were not successful in our hands. In addition to the dimpling problem (Welsh and Schwartz, 1999), the bundles could not be implanted without removing the dura over a substantial portion of the cortical surface. The implantation always provoked profuse cortical swelling. This oedema reaction and associated tissue damage may have been aggravated by the speed of implantation (see Nicolelis et al., 1999). However, even if the implantation was done slowly and the swelling was limited, the use of the micro-wires appeared problematic when they were implanted at a low depth, as is the case when aiming at the granular layer (450 μm under the surface). When the swelling disappeared after a few days, the electrodes floated above the surface, and no signals could be recorded.

The specific challenges associated with ensemble recordings in the cerebellar cortex of awake rats necessitated a new electrode system with individually moveable sharp electrodes with high impedance. The multi-electrode system we designed is lightweight (14 g) and small (base plate: 19 × 23 mm; total height: 16 mm) and allows for the placement of six electrodes, the vertical position of which can be adjusted at any time after implantation. The overall concept was inspired by a single-unit recording device described by Oliveras et al. (1990).

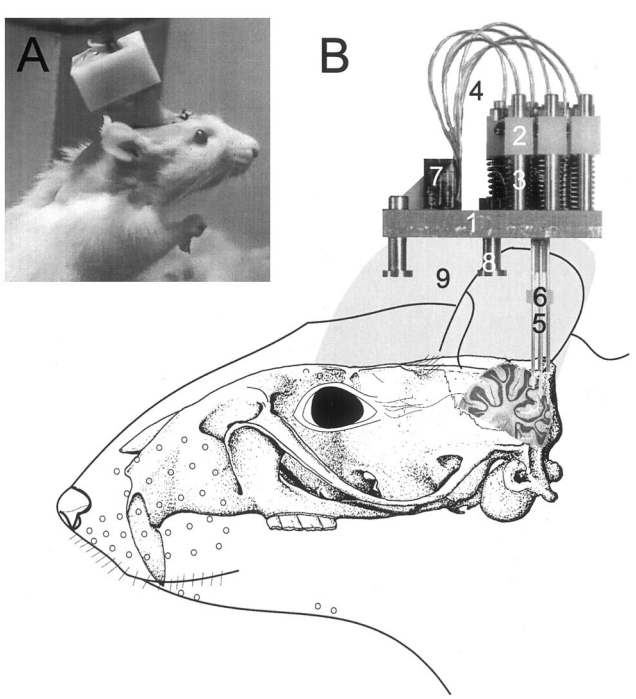


Fig. 1. Implanted multi-electrode carrier, (A) photograph of implanted rat; (B) schematic representation of the implant: 1, base plate; 2, electrode head; 3, sliding bar with spring; 4, connecting wires; 5, electrode guiding tubes; 6, guiding tube matrix; 7, connector; 8, mounting foot; and 9, dental cement.

## 2. Materials and methods

### 2.1. Multi-electrode carrier

#### 2.1.1. Overall concept

The multi-electrode system consists of a base plate on which six stainless steel shafts are mounted vertically in two rows of three around a central circular opening (Figs. 1 and 2). Perpendicular to each shaft, a stainless steel drive screw is screwed into the plate. Each shaft/screw pair is fitted with a plastic element, the 'electrode head', that slides down on the shaft/screw without lateral movement. The vertical descent of the electrode head is prohibited by a spring around the screw. Turning down the screw produces a gradual vertical descent of the plastic electrode head. Each electrode head contains a small-diameter slot in which the electrode can be fitted on the one side, and the electrode-lead to the connector on the other side. This connection is secured by a micro-screw that reaches the middle of the slot in a 45° angle. The circular opening in the center of the base plate is fitted with a plastic cylinder with six small circular openings arranged in a 2 × 3 matrix; they hold the stainless steel electrode guiding tubes (Fig. 3). The matrix arrangement of the guiding tubes is assured by fitting a similar plastic cylinder at the other end of the tubes and by encapsulating it in silicon paste. The base plate also holds the connector to which six insulated lead wires and two silver wires (that are used as reference and ground) were soldered.

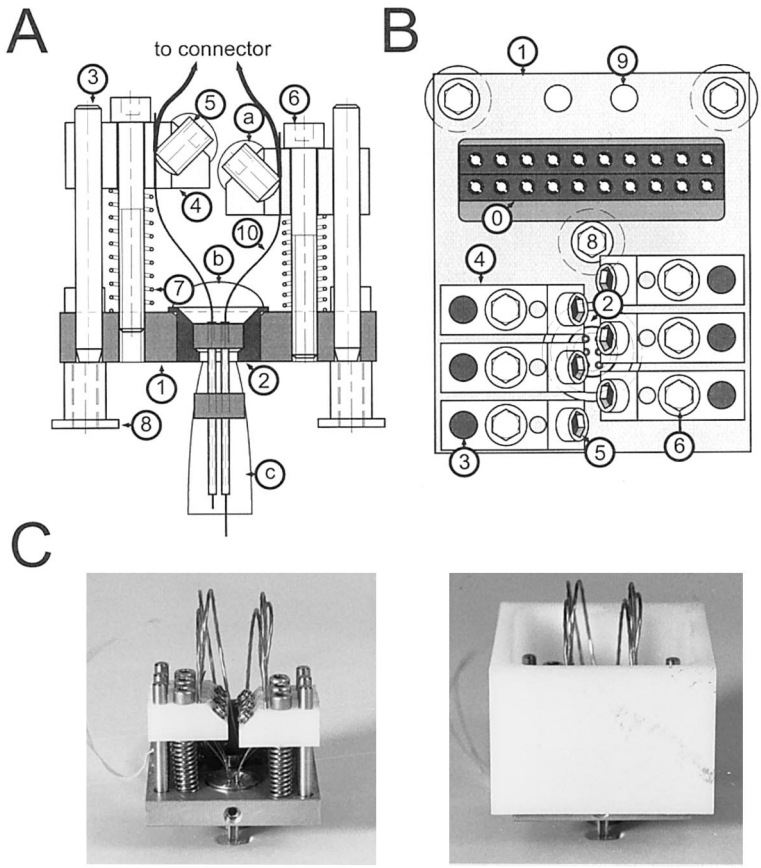


Fig. 2. Electrode carrier; schematic representation of front (A) and top (B) view of the carrier with: 0, connector; 1, base plate; 2, guiding tube matrix; 3, sliding bar with spring; 4, electrode head; 5, electrode securing screw; 6, electrode driving screw; 7, spring; 8, central mounting foot; 9, screw hole for micropositioner arm attachment; 10, connecting wire; a, b, and c: silicon paste. (C) Photographs of the completely mounted carrier with (right) and without (left) POM cover.

### 2.1.2. Construction of the carrier

*2.1.2.1. Base plate, sliding bars, driving screws and mounting feet*. The base plate was made of C36000 free cutting brass (Small Parts, Miami Lakes, FL). The use of this material allows the highest machinability. The low electrical resistance of 6.4 μΩ/cm (Lynch, 1989) prevents potential differences in the plate. The sliding bars were made of precision ground stainless steel shafts with a diameter of 1/16 in. (Ref. O-CGSX-1, Small Parts) cut to a length of 15.5 mm. Before assembly, the shafts were milled to have a conical tip so that they could be pressed more easily in the base plate. The drive screws were 1/2 in. long stainless steel No. 0–80 cap screws with a hex socket head (Ref. O-SHCX-080-8, Small Parts). The mounting foot screws were 3/16 in. long stainless steel No. 0–80 cap screws with a hex socket head (Ref. O-SHCX-080-3, Small Parts). The electrode-restraining screw was a 4 mm stainless steel M2 set screw (model: DIN916) with a size 0.9 hex socket head and a cupped point (Ref. O-MSSX-2-4, Small Parts). In early trials it appeared that the cupped point often cut both electrode and connecting wire, when screwed too tightly. We therefore removed the cupped point on a lathe and made it spherical. The spring was custom coiled from 0.3 mm diameter stainless steel spring wire (12 mm long, 0.6 mm pitch, 2 mm internal coil diameter).

First the brass was milled to a platform of 19 × 23 × 3 mm. On one end of the platform six holes were drilled for the sliding rods and six for the drive screws (see Fig. 2 for positioning of the holes). Subsequently, the six drive screw-holes were tapped for No. 0–80 machine screws. The fine threads resulted in a movement of 317.5 μm/rotation. The six holes for the sliding bars were reamed to 1.58 mm. Central to the six drive screw holes, a 5 mm opening was drilled for the guiding tube matrix. In the back of the platform a 2.3 mm deep, 16 × 5 mm slot was milled for the connector. Three additional 1.6 mm holes were drilled for the screws of three mounting feet: one central to the connector slot, and two in each corner behind the connector slot (Fig. 2). Just behind the connector slot, another two holes were drilled for attachment of the carrier to the micropositioner (Fig. 2). In the front side of the platform (see Fig. 2C), a 1.6 mm hole was drilled and tapped for

another M2, DIN 916 screw (Small Parts) that served to restrain the guiding tube matrix. Prior to assembly, the base plate was gold plated (not polished) to provide protection against corrosion.

*2.1.2.2. Guiding tube matrix*. The guiding tube matrix consisted of six stainless steel tubes positioned in a $2 \times 3$ matrix (Fig. 3). The matrix configuration was obtained by fitting the tubes in two plastic grids. These grids were made from 1.5 mm thick polyacetal homopolymere (POM, Delrin®, obtained from Small Parts) discs (3 mm diameter). In both discs, two rows of three 0.45 mm holes, were drilled at 0.8 mm intervals.

The guiding tubes were sawed with a scalpel from small bore welded tubing (type 304W, 27 gauge, 0.008 in. inner, and 0.016 in. outer diameter; Small Parts). After cutting the tubes to a length of 10 mm, they were deburred internally with a hypodermic 24 gauge needle and inspected with a microscope. The six guiding tubes were fitted in the two plastic grids (see Fig. 3A for positioning) and permanently fixed using cyanoacrylate.

In order to position the guiding tube matrix in the central opening in the base plate, this opening was fitted with a 3.1 mm diameter, 2.5 mm deep stainless steel chamber (Fig. 3). This cylindrical chamber was turned on a lathe. The topside of the chamber had an outward edge (0.3 mm) that rested on the base plate, and an inner edge (0.3 mm) which served to hold the plastic grid with the guiding tubes. The position of the grid with the guiding tubes in the chamber was secured by applying a droplet of melted dental wax to the bottom of the base plate between the chamber and the upper plastic grid. The chamber, fitted with the guiding tube matrix was locked to the base plate by tightening the M2 DIN 916 screw in the front side of the base plate.

*2.1.2.3. Electrode head, connecting wires and connector*. The electrode heads (see Fig. 2) were made of POM. Small blocks ($8.6 \times 3 \times 4$ mm) were milled. In the top surface three holes were drilled: one for the sliding bar (1.59 mm diameter) one for the drive screw (1.51 mm diameter) and one for the electrode/connecting wire (1 mm diameter) (see Fig. 2B for positioning). The top corner closest to the electrode/connecting wire-hole was milled to form a $3 \times 3$ mm platform in a 45° angle (see Fig. 2A). In the middle of this angled platform a 1.6 mm hole was drilled towards the hole of the electrode-connecting wire. This angled opening was tapped to hold the M2 DIN 916 electrode securing screw.

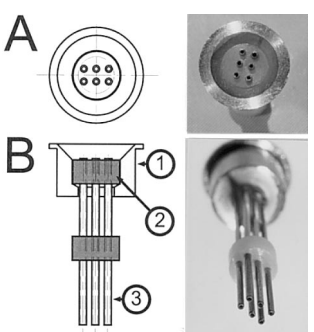


Fig. 3. Schematic representation and photographs of guiding tube matrix. (A) Top view. (B) Front view. 1, guiding tube matrix; 2, plastic grid; and 3, guiding tube.

The connection between the 20-hole connector (DB-25, NB-Labs, Denison, TX) and the electrodes was made by fine, plain copper, stranded conducting wires with a PVC-sheath, soldered to the first six connector leads (the remainder of the 16 recording channels were not used). Teflon coated silver wires (reference and ground; 125 μm diameter) were soldered to the appropriate connector leads. Once all wires were soldered to the leads, the connector was fitted in the slot on the base plate with epoxy resin (Permabond Mix and Fix Two part epoxy resin, Permabond, Eistleigh, UK). After curing of the epoxy, the isolation of the connector leads from the base plate was tested.

*2.1.2.4. Electrodes*. In the experiments described in this paper, we used two types of sharp, tungsten microelectrodes.

The first two carriers were equipped with tungsten microelectrodes with a thin parylene coating (1 μm tip, 127 μm shaft diameter) and an impedance of 2 MΩ (World Precision Instruments, Stevenage, UK). Although these electrodes gave suitable results during the first recording session, the parylene coating did not withstand repeated movement of the electrode through the guiding tubes. Once the electrode position was adjusted a few times, the edges of the cannula scratched the parylene coating of the electrode, producing a false contact between electrode and shaft, which resulted in the loss of suitable signals. In the second and third carrier, we therefore applied silicon paste to the ends of the guiding tubes (see further), and used tungsten electrodes (1 μm tip, 125 μm shaft diameter) with an epoxylite insulation, and impedances ranging from 10 to 12 MΩ (UEWLEESELN1J/85mm, Frederick Haer, Bowdoinham, ME).

*2.1.2.5. Loading of the electrodes*. The base plate was completely assembled as shown in Fig. 2 before loading the electrodes.

First, both the top and the bottom of the guiding tubes were covered with a droplet of silicon paste. We used a non-acidic silicone RTV adhesive (Dow Corning 3140 MIL-A-46146 RVT, purchased from World Precision Instruments, Stevenage, UK) which is non-corrosive and does not release acidic acid during curing (curing times at room temperature were 10–20 min). When applying the paste to the guiding tube ends,

scrap-electrodes were placed in the tubes to prevent them from being clogged. After curing, the silicon drops stayed clear and translucent and were very soft.

The hardened silicon blob at the bottom of the tube openings was cut (with a scalpel blade) to form a flat surface. The translucent silicon allowed for each of the guiding tube openings to be clearly visible. In addition, the silicon drops were soft enough to let the electrodes pass smoothly but were viscose enough to keep them in place during the loading process. Once the end of the electrode reached the top of the guiding tube, the electrode was pulled upward to the point where the electrode tip at the bottom of the guiding tube was completely covered by the silicon drop. The POM electrode head was then slid over the electrode and positioned over the corresponding sliding bar, and the driving screw was screwed in the base plate. Again, the viscosity of the silicon drops prevented the electrodes from sliding out of the tubes, which made correct positioning of all electrodes (all tips at same distance from the guiding tubes) fairly easy. The electrode ends were cut at the top of the plastic electrode heads with microscissors, and the epoxylite insulation gently stripped for a few millimeters. The PVC-covered connecting wires that were stripped and enforced with a droplet of tin/alloy solder were then placed in the electrode hole. The M2 DIN 916 electrode securing screw was then tightened to provide a good contact between the electrode and connecting wire, locking them to the electrode head. The securing screws, as well as the cut end of the electrode were sealed with a drop of silicon paste. The silicon paste was applied to the socket head and to the cut electrode end using a 1 ml syringe with a 24-gauge hypodermic needle.

The bottom of the base plate was covered with paper tape to prevent the dental cement from attaching to the plate, so that recovery of the plate was easier after use. In addition, a droplet of silicon paste was applied to each of the six holes of the electrode driving screws at the bottom side of the base plate. The preparation of the electrode carrier was completed by attaching three mounting feet to the base plate. Before the implantation surgery, the carrier was attached to the arm of a Kopf micropositioner.

### 2.2. Subjects and housing conditions

Female laboratory rats (Rattus Norvegicus) of the Sprague–Dawley strain (IFFA CREDO BELGIUM, Brussels, Belgium) were used ($n = 4$, 280–320 g). So far, the carrier was used in four different rats. Rats were housed in the animal facility of the Faculty of Medical and Pharmaceutical Sciences at the University of Antwerp. Before the surgery they were housed in standard plexi-glass cages with a soft bedding and food and water available ad libitum. Post-operatively, they were transferred to cages with a higher cover-top. The day–night cycle was not reversed.

### 2.3. Implantation surgery

Surgical procedures were carried out in an aseptic environment using sterilized surgical tools. The fully assembled electrode-carrier was gas sterilized. Rats were anesthetized with an intraperitoneally (i.p.) injected mixture of ketamine HCl (75 mg/kg; Ketalar, Parke–Davis, Warner Lambert Manufacturing, Dublin, Ireland) and xylazine HCl (3.9 mg/kg; Rompun, Bayer AG, Leverkusen, Germany) in normal saline (0.9% NaCl, Baxter nv, Lessine, Belgium). Supplemental doses (1/3th of initial dose, injected intramuscularly) were given every 2 h to maintain anaesthesia. The heart rate was monitored (Hewlett–Packard 78342A, Boeblingen, Germany) and toe-pinch reflexes were assessed to control the level of anaesthesia.

The rat's head was fixed in a Kopf stereotaxic frame (David Kopf Instruments, Bilaney Consultants GmbH, Düsseldorf, Germany) with unsharp earbars that do not pierce the eardrum and a standard mouth piece with incisor bar. A homeothermic blanket system (Harvard Apparatus, South Natick, MA) was used to maintain core temperature (37–38°C).

A midline incision was made and the entire skull surface was exposed and freed from connective tissue. Dorsal cranial muscles were removed to expose the caudal part of the skull and the first cervical vertebrae. Eight stainless steel microscrews (Fine Science Tools GmbH, Heidelberg, Germany) were tapped in the skull to serve as anchors for the dental cement. They were arranged in two parasagittal rows of four (one on each side) so that each skull plate held at least two screws (two rostral to Bregma, two caudal to the lambdoid suture, and four in between). The bone screws were covered with cyanoacrylate and then with a layer of dental cement (Hygenic Repair Resin, The Hygenic Corporation/Akron, OH). Four small wholes were drilled to allow fixation of the reference and ground wires and temporarily covered with sterile bone wax (Ethicon, Johnson and Johnson International, Brussels, Belgium). On the left side, the squamous part of the occipital bone was removed to make a $5 \times 5$ mm opening over Crus I and II of the cerebellum. A Friedman curved bone rongeur and a dental drill were used for the craniotomy. A temporary saline drip was installed to keep the dura moist. The tip of a 29-gauge injection needle was bent in a 90° angle and used as a microknife to incise, reflect and remove the dura. Immediately after dura removal, warm (35°C) AGAR (2% in 0.1 M phosphate buffered saline) was placed over the exposed cerebellar surface. Before placement of the electrode carrier, the incisor bar was removed and the rat's head was tilted downward to level Crus II almost

horizontally. Before the carrier was placed in the final position, the two silver wires (ground and reference) were placed under the skull through the aforementioned holes. After removal of the Agar, the carrier was placed in its final position using a standard Kopf micro-positioner. The carrier was positioned so that the six silicone-covered electrode guiding tubes were aligned in three transversely oriented rows of two (or two parasagitally oriented columns of three). The flattened surface of the silicon cover was lowered until it touched and levelled the cerebella surface so that the cerebella cortex was stabilized and its curvature reduced. These measures improve the stability of the recordings (Welsh and Schwartz, 1999). Once the carrier was in place, the skull opening was sealed off with bone wax. The carrier was fixed to the skull with dental cement. The skin incision was closed in layers and surgical antibiotic powder (neomycin) was spread over the head wound.

Immediately after the surgery, an i.p. injection of 0.075 mg/kg buprenophine was given. For further post-operative pain management, rats received subsequent i.p. injections of buprenorphine, every 12 h for the next 3 days. Weight evolution was determined daily to assess recovery.

### 2.4. Recording procedure

Recordings started at least 6 days after the surgery. The recordings described in the present text were carried out to test the validity and reliability of the electrode carrier to perform chronic recording of multiple single units in the cerebellar cortex in awake, freely moving rats.

The first recording session was performed to find neuronal signals on each of the channels. For this, rats were transported to the laboratory, briefly restrained by wrapping them in a towel, and connected to the recording equipment by plugging two 10-pole head stages (NB-Labs, Denison, TX) to the 20-hole connector on the carrier. The head stages contain field effect transistors (Motorola MMBF5459) that are set as voltage followers with unity gain (for full description see Nicolelis et al., 1999). Once the connection was made, the rat was placed in a plexiglas observation box ($L = 40 \times W = 40 \times H = 30$ cm) without bedding where it could move freely. A hook attached to a flexible arm and centred above the observation box held up the insulated cables that connect the head stages to the MNAP-preamplifier (see further). A high resolution CCD color camera (Euromex, Arnhem, The Netherlands) hooked up to a videorecorder (Panasonic NVSD430) and a high resolution color monitor (Panasonic WV-CM 1470) were used to videotape the behavioral activity of the rat.

After a habituation period of 5 min, the rat was again gently restrained to allow the experimenter access to one of the carrier-screws. Screws were turned extremely slowly downward (quarter turn: about 75 μm, every 15 min) until a suitable neuronal signal was obtained. It should be noted that until each channel showed acceptable signals, the rat needed to be restrained again and again, and the electrodes moved at each instance. It is therefore necessary to habituate the rat to the restraining procedure long before the implantation of the carrier. The better the rat is habituated, the longer a gentle restraint is possible, and the more time can be taken for a slow positioning of the electrodes.

### 2.5. Testing of the stability of the recorded waveforms

On the first test day, three separate 20 min recordings were done after all channels showed well-discriminated waveforms. To synchronize the videotape recording of the behavior, the start of the neuronal recording was indicated with a flashing light cue.

In order to test waveform stability, rats underwent the same procedure 2 days after the first recording session. Electrode positions remained unchanged. Again three separate 20 min recordings were performed.

### 2.6. Multi-channel signal processing electronics and analysis software

Microelectrode signals were amplified and filtered (gain = 5000–15 000; bandpass = 400 Hz to 20 kHz), digitized and discriminated with a PC-controlled Multi-channel Neuronal Acquisition Processor (MNAP, Plexon, Dallas, TX). The set-up we used has 16 active channels (which is the minimal set-up), of which only six are used. For a full description of the signal processing electronics of this system we refer to a recent text of Nicolelis et al. (1999). The discrimination of spike waveforms was done using a real-time hardware-implemented combined time/voltage window discriminator, that is part of the RASPUTIN-software package that controls the MNAP (Plexon). Raw and discriminated signals were displayed on an oscilloscope (BK Precision 2120, Maxtec International, Chicago, IL) and fed through an audio monitor (Grass AM8, Astro-Med, West Warwick, RI) for further inspection. Waveforms and recorded spike trains (time series) were stored on computer disk for off-line analyses. For off-line sorting of digitized waveforms OffLine Sorter (Plexon) was used. Spike train analyses were performed using NeuroEXplorer (NEX Technologies, Winston–Salem, NC) and MATLAB (The MathWorks, Natick, MA). Vos et al. (1999a,b) provides a detailed description of the analyses.

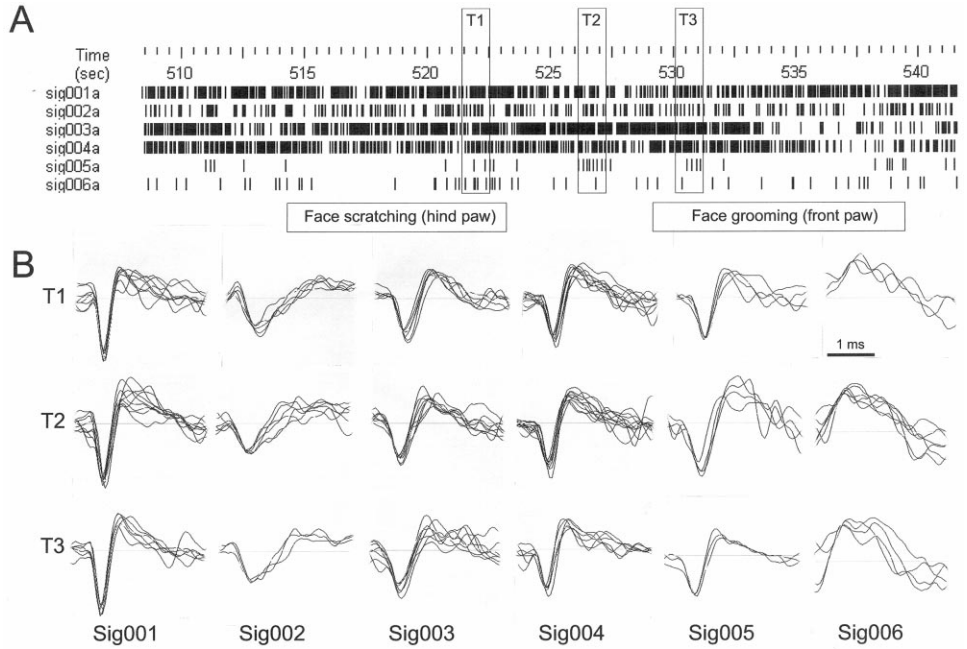


Fig. 4. Stability of recorded waveforms during face scratching and face grooming; (A) rasterized traces of simultaneously discriminated spikes with time of recording noted on top, and episodes of face scratching and face grooming indicated below, three vertical bars (T-1, T-2 and T-3) indicate the time periods during which sampled spikes for each of the six channels (SIG 001–SIG 006) are shown in B.

## 3. Results and discussion

Four rats were implanted with different versions of the multi-electrode carrier. The use of electrodes with a stronger shielding (epoxylite) and the application of silicon RTV adhesive proved to be the improvements which were crucial in making the system suitable for recording well-isolated spike waveforms in awake rats.

Rats seemed to support the system fairly well. In the first days after the implantation they were often observed in a crouched position with the head lying sideways so that the carrier rested on the cage floor. Food and water supply were therefore positioned on the cage floor during the immediate post-operative period, and all rats did eat and drink normally. The abnormal crouching position disappeared a week after the operation and was most likely because of the fact that some neck muscles had been stripped during the surgery and the rat was not capable of supporting the carrier. It is also possible that the carrier was yet too heavy; we have planned several adjustments to reduce the overall weight of the system (i.e. drilling holes in base plate and POM cover). In the observation/recording cage, the rats did not resist the gentle restraint with a towel necessary for the displacement of the electrodes.

In each recording session, little downward movement of the six high-impedance electrodes was necessary to detect neuronal signals with a considerable signal-to-noise ratio on almost all channels (median over all session = 4/6). The mean time to retrieve acceptable signals on 4/6 electrodes was 47 min over all rats/sessions. Purkinje cell complex spikes were clearly detectable (results not shown) and entry into the granular layer was always accompanied by a large increase in the background noise, because of granular cell multi-unit activity.

On each test day, the recorded spikes remained extremely stable throughout subsequent recording sessions that were done for at least 3 h after spike isolation on each of the channels. Also, recorded signals appeared not to be hampered by vigorous movement or mechanical disturbance of the carrier (e.g. produced during face grooming or face scratching, see Fig. 4). In contrast to what was expected, the use of high impedance electrodes did not result in high levels of electronic noise or movement artifacts (Moxon, 1999).

We were, however, not able to keep the same neuronal signals for two subsequent days. In all cases, recorded signals appeared much weaker when the recording was done the next day without moving the electrodes. In some instances a gain increase could bring back a waveform that resembled the one recorded on the previous day (results not shown). In most cases the signals were too weak to be discriminated. Subsequent electrode movement (either up or down) sufficed to again obtain discriminable neuronal signals. We hypothesize that this loss of signal is because of the appearance of scar tissue at the electrode tip. The small tip size of the electrodes we used ($< 1$ μm) did obviously not need much inflammatory foreign body reaction to be nearly completely covered, and consequently loss of function (Nicolelis and Chapin, 1994; Moxon,

1999). We are therefore currently testing broader tipped electrodes in the same impedance range.

## Acknowledgements

The authors wish to thank Inge Bats for the photography. This research was funded by EC contract BIO4-CT98-0182, by IPA Belgium (P4/22) and by the Fund for Scientific Research-Flanders (FWO-Vl) (No. 1.5.504.98). BPV and EDS are supported by the FWO-Vl. We would also like to acknowledge the many useful suggestions of the anonymous reviewers.

## References

Hartmann MJ, Bower JM. Oscillatory activity in the cerebellar hemispheres of unrestrained rats. J Neurophysiol 1998;80:1598–604.

Ito M. The Cerebellum and Neural Control. New York: Raven Press, 1984.

Lynch CT. CRC Practical Handbook of Materials Science. Boca Raton, FL: CRC Press, 1989.

Moxon K. Multichannel electrode design: considerations for different applications. In: Nicolelis MAL, editor. Methods for Neural Ensemble Recordings, CRC Methods in Neuroscience Series. Boca Raton, FL: CRC Press LLC, 1999:25–46.

Nicolelis MAL, Chapin JK. Spatiotemporal structure of somatosensory responses of many-neuron ensembles in the rat ventral posterio-medial nucleus of the thalamus. J Neurosci 1994;14:3511–32.

Nicolelis MAL, Stambaugh CR, Brisben A, Laubach M. Methods for simultaneous multisite neural ensemble recordings in behaving primates. In: Nicolelis MAL, editor. Methods for Neural Ensemble Recordings. Boca Raton, FL: CRC Methods in Neuroscience Series, CRC Press LLC, 1999:121–56.

Oliveras JL, Martin G, Vos B, Montagne J. A single-unit recording system, contact thermal probe and electromechanical stimulator for studying cellular mechanisms related to nociception at brain stem level of awake, freely moving rats. J Neurosci 1990;35:19–29.

Vos BP, Volny-Luraghi A, Maex R, DeSchutter E. Parallel fibers synchronize spontaneous activity in cerebellar golgi cells. J Neurosci 1999a;19(RC6):1–5.

Vos BP, Volny-Luraghi A, De Schutter E. Cerebellar Golgi cells in the rat: receptive fields and timing of responses to facial stimulation. Eur J Neurosci 1999b;11:2621–34.

Vos BP, Volny-Luraghi A, Maex De Schutter E. Precise spike timing of tactile-evoked cerebellar Golgi cell responses: a reflection of combined mossy fiber and parallel fiber activation. Progress Brain Res 1999c: in press.

Welsh JP, Schwartz C. Multielectrode recording from the cerebellum. In: Nicolelis MAL, editor. Methods for Neural Ensemble Recordings. Boca Raton, FL: CRC Methods in Neuroscience Series, CRC Press LLC, 1999:79–100.

Wilson MA, McNaughton BL. Dynamics of the hippocampal ensemble code for space. Science 1996;261:1055.